Two Different Zinc Sites in Bovine 5-Aminolevulinate Dehydratase Distinguished by Extended X-ray Absorption Fine Structure†

Andrew J. Dent,‡ Detmar Beyersmann,§ Christoph Block,§ and S. Samar Hasnain*,‡

Synchrotron Radiation Research Division, Daresbury Laboratory, Warrington WA4 4AD, U.K., and Department of Biology and Chemistry, University of Bremen, D-2800, Bremen 33, West Germany

Received October 24, 1989; Revised Manuscript Received February 28, 1990

ABSTRACT: The zinc coordination in 5-aminolevulinate dehydratase was investigated by extended X-ray absorption fine structure (EXAFS) associated with the zinc K-edge. The enzyme binds 8 mol of zinc/mol of octameric protein, but only four zinc ions seem sufficient for full activity. We have undertaken a study on four forms of the enzyme: (a) the eight-zinc native enzyme; (b) the enzyme with only the four zinc sites necessary for full activation occupied; (c) the enzyme with the vacant sites of (b) occupied by four lead ions; (d) the product complex between (b) and porphobilinogen. We have shown that two structurally distinct types of zinc sites are available in the enzyme. The site necessary for activity has an average zinc environment best described by two/three histidines and one/zero oxygen from a group such as tyrosine or a solvent molecule at 2.06 ± 0.02 Å, one tyrosine or aspartate at 1.91 ± 0.03 Å, and one cysteine sulfur at 2.32 ± 0.03 Å with a total coordination of five ligands. The unoccupied site in (b), obtained by taking the difference spectrum between the spectra from samples (a) and (b), is dominated by a single contribution of four cysteinyl sulfur atoms at 2.28 ± 0.02 Å. Spectra from samples (c) and (d) show only small changes from that of (b), reflecting a slight rearrangement of the ligands around the zinc atom.

The zinc enzyme 5-aminolevulinate dehydratase (ALAD,[1] 5-aminolevulinate hydro-lyase, also called porphobilinogen synthase, EC 4.2.1.24) catalyzes the synthesis of the pyrrole porphobilinogen from two molecules of 5-aminolevulinic acid. The enzyme from bovine liver has a molecular mass of 280000 Da and consists of eight subunits of 35000 Da each (Shemin, 1976). Only half of the subunits seem to be involved in catalysis, since the trapping of 4 mol of substrate/mol of octameric protein by reduction of Schiff base intermediates led to nearly total enzyme inactivation (Jaffe & Hanes, 1986). The isolated enzyme binds a maximum number of eight Zn^{2+} per octamer with high affinity (Tsukamoto et al., 1979; Bevan et al., 1980; Sommer & Beyersmann, 1984). The zinc chelators EDTA and 1,10-phenanthroline reversibly inhibit the enzyme, and full activity may be restored by binding four Zn^{2+} ions per octamer (Bevan et al., 1980). Also, the protein deprived of zinc by the reversible thiol modifier methylmethanethiosulfonate requires only four Zn^{2+} (or Cd^{2+}) per octamer for full catalytic activity (Jaffe et al., 1984). Although one laboratory (Tsukamoto et al., 1980) reported the necessity of the full equivalent of eight bound Zn^{2+} per octamer for maximum activity, the other results suggest that there exist two different zinc sites in the octamer and that the occupation of half of the eight sites suffices for the catalytic function. The enzyme is inhibited by Pb^{2+} ions at micromolar concentrations; the stoichiometry of the inhibited complex is not known (Cheh & Neilands, 1976).

Lysine, histidine, and cysteine have been identified as amino acid constituents of the enzyme protein involved in the active site (Shemin, 1972; Chaudhry et al., 1976; Tsukamoto et al., 1979). Two cysteine residues essential for the enzyme activity are rapidly oxidized by air, and the maintenance of the active site requires the presence of a thiol (Batlle et al., 1967). Recently, the sequence of a cDNA clone for human ALAD has been elucidated (Wetmur et al., 1986). The corresponding deduced amino acid sequence is collinear with the amino acid sequences of fragments of the bovine enzyme including a 44 amino acid N-terminal fragment. A cysteine- and histidine-rich sequence (119–132) corresponds to a consensus sequence for the so-called zinc fingers in many zinc proteins (Berg, 1986).

In a previous EXAFS study various forms of bovine ALAD with all eight zinc sites occupied were investigated (Hasnain et al., 1985). The study of the native enzyme suggested that the zinc environment consisted of three sulfur atoms at 2.28 ± 0.02 Å and a lower *Z* atom (N or O) at 1.92 ± 0.05 Å. The results, when combined with previous findings, were taken to indicate that zinc may only have a structural role rather than a direct catalytic role in ALAD.

We have undertaken a further study on four forms of the native enzyme: (a) the eight-zinc enzyme (hereafter referred to as Zn_8); (b) the enzyme with only the four zinc sites necessary for full activation occupied (Zn_4); (c) the enzyme with the vacant sites of (b) occupied by four lead ions (Zn_4Pb_4); (d) the Zn_4 enzyme–product complex (Zn_4PBG).

Materials and Methods

Materials. Water was bidistilled over quartz. All salts were of analytical grade (p.a.). 2-Mercaptoethanol and Fractogel TSK-DEAE-F were obtained from Merck (Darmstadt, West Germany). Porphobilinogen and Tris base (TRIZMA) were purchased from Sigma (Deisenhofen, West Germany), and DEAE-Sephacel and octyl-Sepharose were acquired from Pharmacia (Uppsala, Sweden). Chelex 100 was from Bio-Rad (München, West Germany). The CF25 ultrafiltration cones

† This work was supported by a travel grant from Deutsche Forschungsgemeinschaft to D.B. We thank the Science and Engineering Research Council for provision of the Facilities at Daresbury Laboratory, for financial support (to S.S.H.), and for the award of a grant to A.J.D.

‡ Daresbury Laboratory.

§ University of Bremen.

[1] Abbreviations: EXAFS, extended X-ray absorption fine structure; ALAD, 5-aminolevulinate dehydratase; PBG, porphobilinogen.

0006-2960/90/0429-7822$02.50/0

Table I: Zinc Content and Specific Activity of the Samples

sample	Zn content (Zn/octamer)	sp act. (nkat/mg)
Zn_8	8.0	1.5
Zn_4	4.3	1.5
Zn_4Pb_4	4.0	1.05
Zn_4PBG^a		

[a] Same sample as Zn_4 supplemented with PBG.

were from Amicon (Witten, West Germany).

Enzyme Purification. The enzyme was purified by a modification of the method of Hasnain et al. (1985). All operations were performed at 4 °C unless otherwise specified. The standard buffer was 50 mM Tris-HCl, pH 7.2, containing 40 mM 2-mercaptoethanol and 10 μM zinc acetate. A total of 800 g of bovine liver was homogenized in an Omni-Mix (Sorvall) with standard buffer and centrifuged at 20000*g*. The supernatant was concentrated by $(NH_4)_2SO_4$ precipitation (at 60% saturation) and redissolution in and dialysis against the standard buffer. The sample was further purified by chromatography on DEAE-Sephacel, which was eluted with a 600-mL gradient of 50–500 mM of Tris-HCl buffer, pH 7.2. The active fractions were concentrated by precipitation with $(NH_4)_2SO_4$ and redissolved in standard buffer containing 30% $(NH_4)_2SO_4$, applied on an octyl-Sepharose column, and eluted by a 600-mL gradient of 30–0% $(NH_4)_2SO_4$ in standard buffer. The active fractions were concentrated by precipitation with $(NH_4)_2SO_4$ and redissolution in and dialysis against standard buffer. The final step was high-resolution Fractogel TSK-DEAE chromatography. The enzyme was eluted by a stepwise gradient of 0–400 mM KCl in standard buffer. The purified enzyme was concentrated with type CF25 Amicon ultrafiltration cones.

Determination of the Enzyme Activity and Protein Concentration. The enzyme was assayed by the method of Mauzerall and Granick (1956). The protein concentration was determined according to Lowry et al. (1951). The properties of the purified enzyme were purification 700-fold and sp act. 1.5 nkat/mg. The final enzyme concentration for recording the EXAFS spectra was 0.55 mM octamers. For preparation of enzyme containing stoichiometrically controlled amounts of zinc or lead, the enzyme was partially zinc depleted by application to a Chelex 100 column and titrated with zinc or lead afterward. The metal content was determined by flame atomic absorption with a Perkin-Elmer Model 2380 spectrophotometer. The preparations containing four and eight Zn^{2+} per octameric protein, respectively, had the same specific activity. Solutions of the concentrated enzyme were very stable, and no significant decrease in activity occurred on exposure of the enzyme, maintained at room temperature, to synchrotron radiation for 24 h. The zinc content and activities of the samples are given in Table I.

Measurement and Interpretation of the EXAFS. EXAFS spectra were recorded at the Zn K-edge (9.661 keV) as fluorescence excitation spectra by use of the fluorescence detection system (Hasnain et al., 1984) at the Daresbury Synchrotron Source on Wiggler station 9.2. The SRS was operating at an energy of 2.0 GeV with an average current of 100 mA. An order-sorting Si(220) monochromator was used to minimize harmonic contamination in the monochromatic beam. A 5-μm Cu foil was placed in front of the 90° in-plane detector and 15-μm foils were placed in front of the other detectors to improve the fluorescence to scattered radiation ratio. Five 75-min scans were collected at room temperature for the Zn_4 sample, three for the Zn_8 sample, and one each for the Zn_4Pb_4 and Zn_4PBG samples. The data were collected with an integration time increasing approximately as a function of k. This together with the improved X-ray intensity of the SRS Wiggler station compared to dipole station 7.1 and the SRS operating at 2.0 GeV as opposed to 1.8 GeV, gave spectra with an order of magnitude better signal to noise ratio, particularly at $k > 9$ Å^{-1}, than that obtained in our previous study a few years ago (Hasnain et al., 1985).

The raw experimental data from each detector were weighted according to the edge height and then averaged and energy calibrated with the Daresbury EXCALIB program (Morrel et al., 1989). Preedge and postedge background subtraction was performed with the Daresbury EXBACK program (Morrel et al., 1989), which employs a polynomial form for the smoothly varying atomic absorption coefficient. The EXAFS thus obtained was normalized to a unit zinc atom and converted to k space.

Transmission EXAFS data were collected at 77 K on the model compounds tetrakis(imidazole)zinc(II) diperchlorate $[Zn(imid)_4(ClO_4)_2]$, hexakis(imidazole)zinc(II) dichloride $[Zn(imid)_6Cl_2)]$, and $[Zn(S\text{-}2,3,5,6\text{-}Me_4C_6H)_2(1\text{-methylimidazole})_2]$. This latter compound is of type $[Zn(SR)_2(imid)_2]$ and hence has a $[Zn(Cys\text{-}S)_2(His)_2]$-type core structure. Transmission EXAFS data on bis(thiourea)zinc acetate $[Zn(SC(NH_2)_2)_2(CH_3COO)_2]$, which has a $[Zn(SR)_2(OR)_2]$-type core structure, was supplied by Dr. G. P. Diakun.

Data analysis utilized rapid curve wave single and multiple scattering theory (Gurman et al., 1984, 1986) in the program EXCURV88 (Binsted et al., 1988) on the raw (i.e., unfiltered) k^3-weighted EXAFS data. Phases shifts were calculated with the MUFPOT program (Pendry, 1974) and within EXCURV88. The programs construct a complex muffin-tin potential from close-packed elemental neutral atom charge densities. The atomic charge densities are calculated with Clementi–Roetti wave functions. The charge overlap is treated with the Matheis (1964) prescription of overlapping charge densities and exchange using the Slater X_α method with an exchange parameter of 2/3. It has been found that the excited central atom is best approximated by the wave functions of a $Z + 1$ atom (in this case gallium) with one electron from the 1s orbital removed. However, when these phase shifts were applied to the model compounds, large errors (≈0.05 Å) in the Zn–N first-shell distance resulted. This is shown in the second and third rows of Table II. Phase shifts calculated with no correction for the central excited zinc atom gave smaller errors (≈0.02 Å) as shown in the fourth row of Table II. At present, we do not understand the reasons for this apparent superiority of the nitrogen phase shift calculated with no correction to the central atom.

The Zn–N distance was then fixed at the X-ray value of 2.00 Å for $[Zn(imid)_4(ClO_4)_2]$ and the N phase shifts were refined by an empirical method within the EXCURV88 program. When these were transferred to the other model compounds, including the model with mixed imidazole and sulfur ligands, accurate first-shell distances resulted as shown in row four of Table II. Further, transferring the zinc phase shifts to the bis(thiourea)zinc acetate data gave Zn–O and Zn–S distances within 0.01 Å of their X-ray crystal values (Cavalca et al., 1967). Thus, we have used these phase shifts, uncorrected for the excited central zinc atom, for the calculations presented in the rest of this paper.

Analysis of these models also provided an amplitude reduction factor due to multielectron absorption of 0.7. The imaginary part of the photoelectron self-energy was set to −1 eV to reproduce the elastic electron mean free path. The photoelectron energy zero E_0 was treated as a single overall

Table II: Comparison of First-Shell Distances from X-ray Diffraction and EXAFS Showing Effects of Different Phase Shifts on Model Compounds[a]

	$Zn(imid)_4$ (4 N)		$Zn(imid)_6$ (6 N)		$Zn(SR)_2(imid)_2$ (2 N, 2 S)			
	r (Å)[b]	$2\sigma^2$ (Å^2)[c]	r (Å)	$2\sigma^2$ (Å^2)	r (Å)	$2\sigma^2$ (Å^2)	r (Å)	$2\sigma^2$ (Å^2)
X-ray	2.00[d]		2.19[e]		2.05[f]		2.30[f]	
MUFPOT (Z + 1) 1s^1[g]	1.96	0.006	2.15	0.012	2.02	0.014	2.30	0.008
EXCURV88 (Z + 1) 1s^1[g]	1.95	0.005	2.13	0.012	2.01	0.011	2.24	0.008
EXCURV88 Z 1s^2[h]	1.98	0.004	2.17	0.010	2.03	0.007	2.29	0.008
EXCURV88 Z 1s^2[h,i]	2.00	0.003	2.19	0.008	2.05	0.005	2.29	0.007

[a] See text for further details. [b] Interatomic distance, r (Å). [c] Debye–Waller factors, $2\sigma^2$ (Å^2); (σ = root mean square deviation in interatomic distance). [d] Bear et al., 1975. [e] Garrett et al., 1983. [f] Corwin & Koch, 1988. [g] (Z + 1) 1s^1 approximation for the central atom. [h] No correction for central atom. [i] N phase shift refined—see text.

parameter for the multiple-shell fit as this has been found sufficient for cases where the nature of the backscattering atoms is similar. [See, for example, Arber et al. (1989).] Again, this was constrained to values close to those obtained for the model compounds, which were found to lie 15–20 eV above the absorption threshold. Fourier transforms were calculated within the plane wave approximation where they were corrected for the phase shift of the first shell of backscattering atoms. This gives peaks in the Fourier transform approximately at the expected radial distance (Gurman & Pendry, 1976). The Fourier transform was used for the purposes of model building and judging the quality of a fit (Perutz et al., 1982). The quality of the structural model was further assessed by the fit index (FI), defined as

$$\frac{1}{100N_{pt}}\sum_{1}^{N_{pt}}([X_i(\text{calc}) - X_i(\text{expt})]k^3)^2$$

where N_{pt} = number of data points. Statistical criteria based on the F-test (Joyner et al., 1987) were used to test the significance of a minor shell.

In the case of modeling of an imidazole group, all the ring atoms were included since the outer-shell atoms have significant multiple-scattering contributions (Strange et al., 1987), but the internal geometry of the imidazole group was constrained during the refinement (Hasnain et al., 1988). For tyrosine however, the model just included carbon atoms C_1, C_2, and C_6

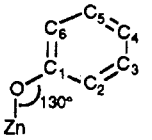

as it has been found from model systems that the outer-shell atoms are too far away from the central atom to make a significant contribution to the EXAFS spectrum (Garratt, 1989; Hasnain & Strange, 1989). Carboxylate linkages were represented just by the first-shell O since no strong multiple-scattering contributions were expected.

Results

Figure 1 shows the XANES spectra for the Zn_4 and Zn_8 samples are distinct, showing significant differences. The EXAFS data, Figure 2, are consistent with this observation. These differences can only be accounted for if two types of zinc sites are present in the octameric enzyme: one type of site is initially occupied for the Zn_4 sample, and the second type of site is occupied when the remaining zinc is added. An alternative explanation requires an interaction between the two types of sites such that the environment of the original four Zn atoms changes upon the addition of a further four Zn atoms. However, the close similarity of Zn_4Pb_4 data to the data of Zn_4 (shown elsewhere in the paper) does not favor this explanation.

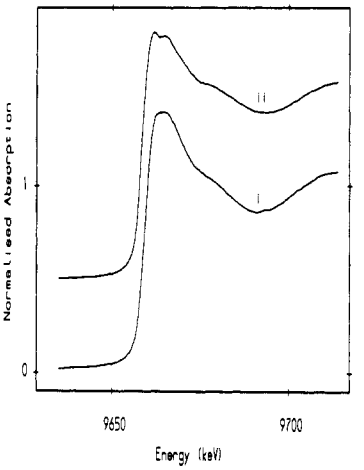

FIGURE 1: XANES spectra for (i) Zn_4 and (ii) Zn_8 samples.

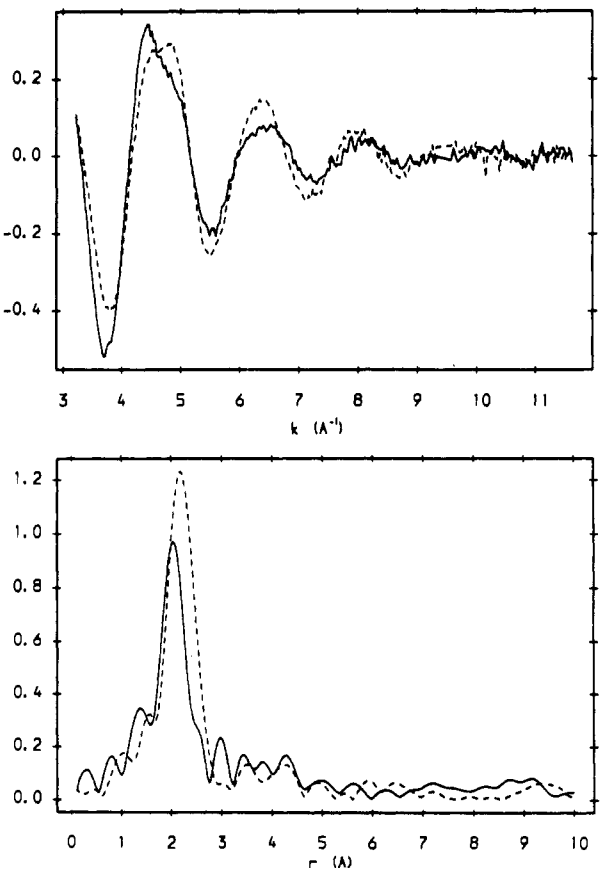

FIGURE 2: Comparison of the k-weighted EXAFS spectra (top) and k^3 Fourier transform moduli (bottom) for Zn_4 (solid line) and Zn_8 (broken line).

Simulation of Zn_4-ALAD (Site A) Data. Figures 3 and 4 show respectively the k^3-weighted EXAFS spectrum and the

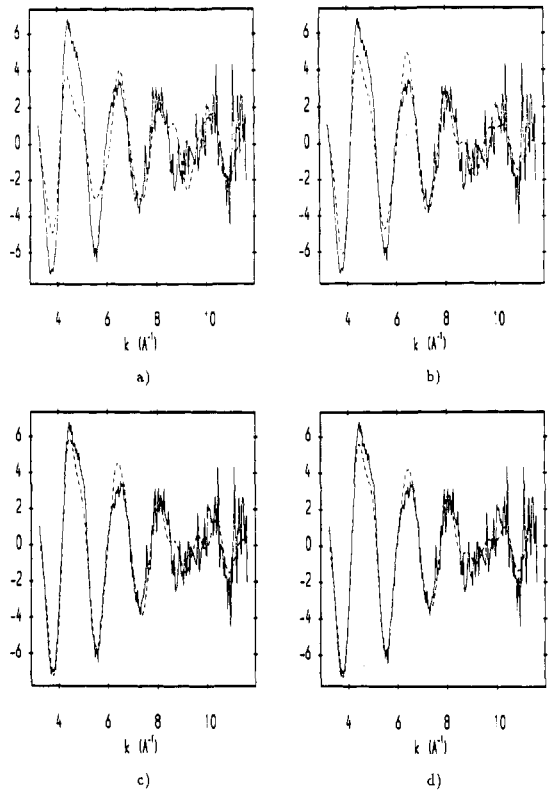

FIGURE 3: k^3 EXAFS spectra of Zn_4 showing the contributions of each of the model components: (a) 3 imid (2.05 Å), FI 6.0; (b) 3 imid (2.05 Å) + 1 cys (2.32 Å), FI 4.0; (c) 3 imid (2.05 Å) + 1 tyr (1.91 Å) + 1 cys (2.32 Å), FI 2.8 (model A); (d) 2 imid (2.05 Å) + 1 tyr (2.07 Å) + 1 tyr (1.91 Å) + 1 cys (2.32 Å), FI 2.7 (model C).

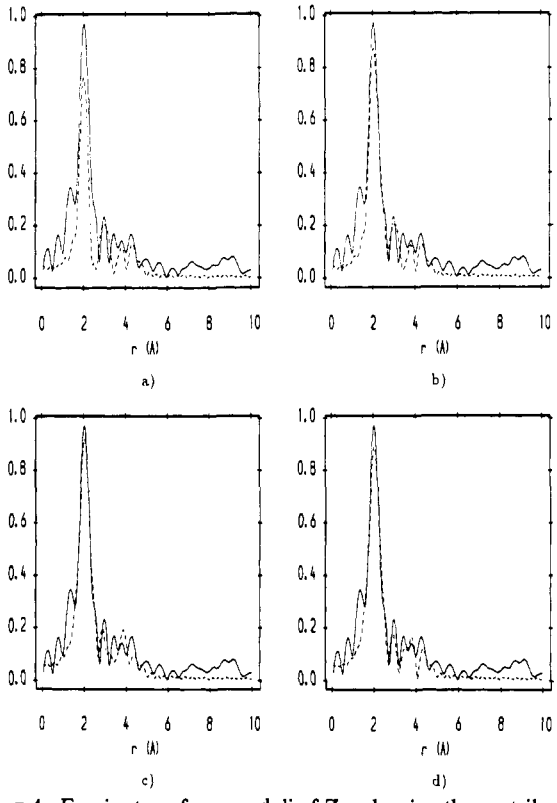

FIGURE 4: Fourier transform moduli of Zn_4 showing the contributions of each of the model components. For details, see Figure 3.

Fourier transform modulus of the Zn_4 sample. The outer-shell peaks in the Fourier transform and the beat pattern in the EXAFS data at $k \approx 4$–6 Å^{-1} are typical of ring groups such as histidine imidazole (Strange et al., 1987) and tyrosine (Garratt, 1989). An analysis of the inner shell shows that the dominant contribution is due to low-Z atoms such as N or O. Figures 3a and 4a show the best simulation with three imidazole ligands at ≈2.05 Å. Refinement with two or three imidazole groups gave equally good simulation to the EXAFS data. However, the Debye–Waller factors became negative (a physically impossible possibility) with the model based on two imidazoles, indicating the presence of other ring residues (tyrosine) or a third imidazole to give three such residues in total. It has been shown previously that a distinction between two- and three-ring residues such as imidazole is possible due to the multiple scattering from the outer-shell carbon atoms (Strange et al., 1987).

Table III: Residues Used in Construction of Models A, B, and C

	ligand distance (Å)			
model	2.05	2.05	1.9	2.3
A	3 His		1 Asp	1 Cys
A	3 His		1 Tyr	1 Cys
B	2 His	1 Asp	1 Tyr	1 Cys
B	2 His	1 Tyr	1 Asp	1 Cys
C	2 His	1 Tyr	1 Tyr	1 Cys

The presence of a heavier scatterer such as sulfur was found at an early stage of the analysis. Inclusion of a single sulfur atom at around 2.3 Å improved the fit index by 40%. This can be seen in Figures 3b and 4b. Detailed first-shell analysis of the EXAFS data shows that the Zn site is five coordinate with at least three components, two from scattering corresponding to low-Z atoms (N/O) at 1.91 ± 0.03 and 2.06 ± 0.02 Å and one from S at 2.32 ± 0.03 Å. The outer-shell carbon atoms at ≈3 and 4 Å group together well with a Zn–N distance of 2.06 Å as the histidine imidazole ligand. Similarly, the remainder of the outer-shell carbon atoms group together with a Zn–O distance of 1.91 Å as another likely protein residue, tyrosine or carboxylate. A number of models have been explored in terms of data analysis including the following best models: (A) three imidazoles, one oxygen (either carboxylate or phenolate), and one cysteine sulfur; (B) two imidazoles, one tyrosine, one carboxylate oxygen, and one cysteine sulfur; (C) two imidazoles, two tyrosines, and one cysteine. The construction of the models can be seen more clearly in Table III. Constrained refinement based on the above-mentioned three best models simulates the EXAFS spectrum equally well. As expected, the differences between models B and C are small and not statistically significant. Panels c and d of Figures 3 and 4 show the simulation using models A and C, which yield fit indices within 10% of each other. In the case of model C, a reasonable account of the 3.3-Å Fourier transform peak is made as arising from the outer-shell carbon atoms from the phenolate-type linkage. The contribution due to the 3.3-Å peak in the EXAFS data is only small, and improvements due to this shell can only be appreciated by visual inspection.

Thus, the average Zn environment in the Zn_4-ALAD is best described by two/three histidine imidazole and one/zero tyrosine (or some other oxygen-donating group, either from the protein or solvent) at 2.06 ± 0.02 Å, one tyrosine or aspartate at 1.91 ± 0.03 Å, and one cysteine sulfur at 2.32 ± 0.03 Å with a total coordination of five ligands.

Simulation of the Difference Spectrum and Zn_8-ALAD. The EXAFS data for the Zn_8-ALAD spectrum are distinctly different from those of the Zn_4-ALAD spectrum. The difference EXAFS spectrum and Fourier transform modulus, i.e., Zn_8 enzyme spectrum minus the Zn_4 enzyme spectrum, are shown in Figure 5. The well-defined nature of the difference

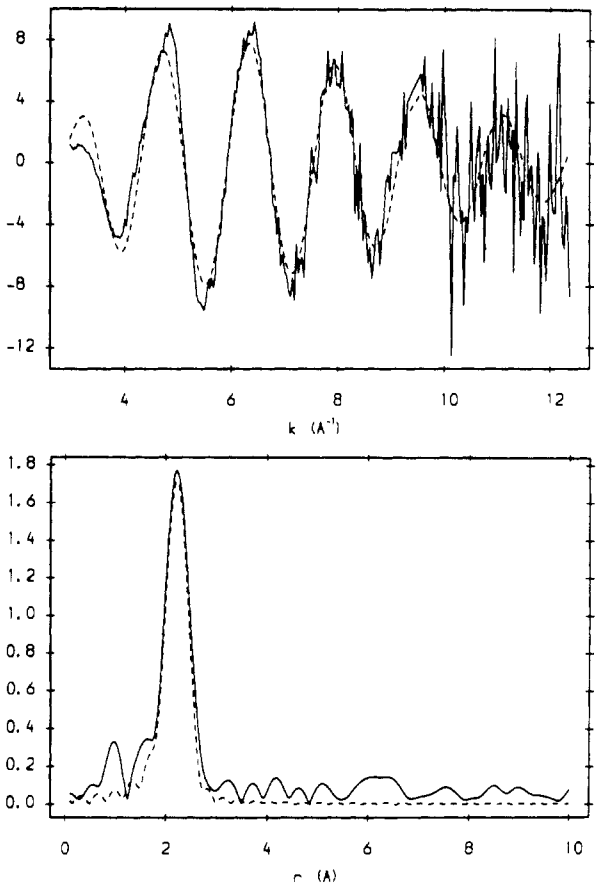

FIGURE 5: k^3-weighted EXAFS spectra (top) and Fourier transform moduli (bottom) for the difference spectrum Zn_B (solid line) and the best-fit model (broken line).

spectrum suggests the existence of two distinct Zn sites in the Zn_8 sample. Analysis of the difference spectrum (from now on called Zn_B) shows that the spectrum is dominated by a single contribution of four sulfur atoms at 2.28 ± 0.02 Å. Further, the Zn_B spectrum resembles closely that from zinc metallothionein where it is known that the Zn atoms are coordinated by four cysteinyl sulfurs (Garner et al., 1982).

The Zn_8 spectrum is very similar to that published earlier (Hasnain et al., 1985) over most of the k region. There is a slight difference between the data in the region k = 3.5–4 Å^{-1}, which may be a result of different biochemical procedures used in the two experiments. In our earlier experiments 9.6 Zn per octamer were present as against 8.0 Zn per octamer (Table I) in the present study. The earlier data were restricted to $k < 9.5$ Å^{-1}, whereas the present data extend to k = 12 Å^{-1}. Both the present and 1985 data are dominated by backscattering from sulfur atoms at ≈2.3 Å, as is borne out by detailed analysis in the two studies.

Zn Environment in Zn_4Pb_4-ALAD. In order to investigate whether the environment of Zn_A sites changes when the last four sites are populated, the Zn K-edge EXAFS of Zn_4Pb_4-ALAD was compared to the Zn_4 and Zn_8 spectra. The close similarity of the Zn_4Pb_4 data to those of the Zn_4 is obvious from Figure 6a. A constrained refinement with Zn_4 model C shows only small changes primarily in the multiple-scattering contribution, reflecting a slightly different geometrical arrangement of the ligands.

Zn Environment in Zn_4-ALAD–Product Complex (Zn_4PBG). Figure 6b shows a comparison of the EXAFS and Fourier transform modulus of the Zn_4 enzyme spectrum and the Zn_4 enzyme–product complex (Zn_4PBG) spectrum. The data for the two samples are very similar, suggesting that the

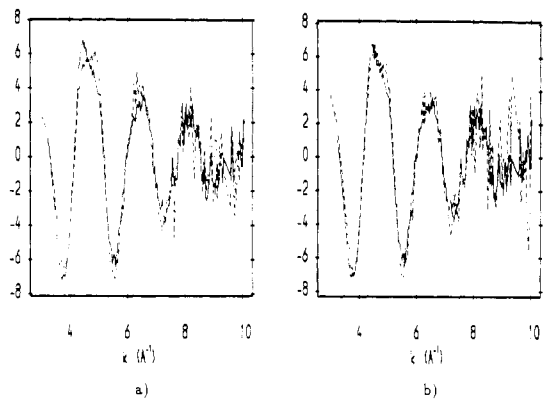

FIGURE 6: Comparisons of the k^3 EXAFS spectra (a) between Zn_4 (solid line) and Zn_4Pb_4 (broken line) and (b) between Zn_4 (solid line) and Zn_4PBG (broken line).

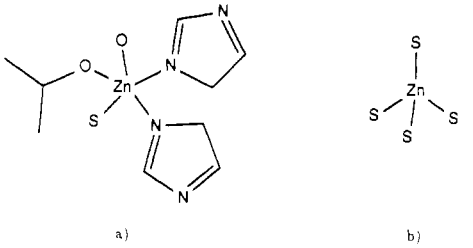

FIGURE 7: Proposed structures of the (a) Zn_A and (b) Zn_B sites. In the Zn_A site oxygen could be from protein ligands (such as aspartate or tyrosine) or from solvent.

Table IV: Structural Parameters Used in the Best Simulation for EXAFS Spectra of Zn_4 (Zn_A)[a] and Zn_B

	Zn_4 (Zn_A)[a]			Zn_B		
ligand	r (Å)	N[b]	$2\sigma^2$ (Å^2)	r (Å)	N	$2\sigma^2$ (Å^2)
Tyr	1.91 (3)	1	0.007			
His	2.05 (2)	2	0.005			
Tyr[c]	2.07 (2)	1	0.005			
Cys	2.32 (3)	1	0.015	2.28 (2)	4	0.012

[a] Model C; refer to Figures 3d and 4d. [b] Number of residues. [c] Other oxygen-donating ligands cannot be ruled out due to its close proximity with the Zn–His obtained here. The carbon atoms in the shell due to these residues lie close to each other and may interfere.

environment of Zn is not perturbed due to substrate binding.

Discussion

Two types of Zn sites have been identified from the EXAFS studies of 5-aminolevulinate dehydratase by use of the difference method between the two different zinc loadings of the enzyme. Table IV summerizes the EXAFS result in terms of the two types of Zn environment. It is not cysteine-rich site B which is occupied preferentially when the apoenzyme is combined with Zn^{2+}, but site A which contributes just one cysteine to the Zn coordination. For site A strong evidence of two/three histidine ligands is found with two/one additional oxygen-donating groups such as carboxylate- or phenolate-type ligands from the protein or water from the solvent. We note that it is only the A sites which are required to be occupied by Zn for the full catalytic activity of ALAD. This evidence, at least, implicates Zn of the site A to be at or near the catalytic center. The nature of ligands for this Zn is typical for a "catalytic" role (Garner & Feiters, 1987). However, the very close similarity of the Zn_4PBG spectrum suggests that Zn itself may not be directly involved with the substrate binding, or if it does, then it induces only subtle changes in the zinc environment.

Figure 7 schematically shows the structures of the two sites. We may ask, what is the biochemical significance of the two

different Zn sites? The most straightforward assumption is that in the Zn_4 enzyme four protein subunits are bound with Zn and in the Zn_8 enzyme each of the eight subunits carries one Zn^{2+} ion. The assumption, i.e., that the fifth to eighth Zn^{2+} are bound to those subunits not occupied in the Zn_4 enzyme, cannot be unambiguously confirmed by our present work, but it is plausible since only one amino acid sequence is known for the protein.

What role may be assigned to Zn_A and Zn_B in the catalytic function of the enzyme? There is no doubt that site A is required to be occupied by Zn for catalytic activity (Bevan et al., 1980; Jaffe et al., 1984). This is consistent with the unambiguous finding that only four substrate molecules are trapped by reduction of Schiff base intermediates in the octamer (Jaffe & Hanes, 1986). In the light of this half-of-the-sites stoichiometry, we propose that at the Zn_A site the metal ion coordinates up to five amino acid residues which are thus oriented in the proper geometry for the active conformation of the four catalytic subunits. These residues are two/three histidines, two/one oxygen linkages such as carboxylate or phenolate, and one cysteine. Interestingly, histidine and cysteine have been inferred from specific covalent modification studies to be catalytic site residues involved in binding with the substrate molecules (in addition to lysine), and these residues have been included in various proposals for the catalytic mechanism [e.g., Barnard et al. (1977) and Schlösser and Beyersmann (1987)]. The latter group suggested that part of the amino acid side groups essential for activity are interacting with Zn and another part with the substrate. This suggestion was based on the amino acid sequence assigned to a "zinc finger" section of the corresponding human protein by Wetmur et al., (1986) and the Zn ligands derived from the first EXAFS investigation on the Zn_8 enzyme by Hasnain et al. (1985). Since the refined EXAFS study described here demonstrates that the EXAFS spectrum of the Zn_8 enzyme represents the average of two types of Zn sites, we have to refine the active site model to accommodate the new data.

We propose that the Zn binding amino acid sequence of the enzyme folds around the Zn ion in two different ways. At site A two/three histidines, two/one aspartate and/or tyrosine or a water molecule, and one cysteine coordinate the Zn_A ions as in the Zn_4 enzyme, whereas at site B four cysteines form the Zn_B sphere. We speculate that at site A the presence of Zn^{2+} is required to fold the catalytic domain in the proper way, whereas at site B Zn^{2+} is not required for activity but stabilizes the native protein, protecting it from denaturation. This interpretation is in concordance with the finding that Zn ions stabilize the enzyme conformation in the presence of urea (Vuga and Beyersmann, unpublished results). How could, in spite of the presence of a single amino acid sequence, four of eight subunits bind Zn^{2+} in a mode differing from that of the remaining four subunits? We assume that four subunits in the octamer interact with the other four subunits in a way that results in different accessibilities of the Zn sites in each two subunits. A model of the quaternary structure of 5-aminolevulinate dehydratase derived from small-angle X-ray scattering describes the octameric protein as a quadratic arrangement of four stacks composed of two subunits each (Pilz et al., 1988). If the contact area of each two subunits within a dimeric stack would involve the Zn site of one of the two subunits only (due to asymmetric association between subunits in dimers), the metal ions would have to accommodate in a differing mode for each of these two subunits. A similar symmetry association between identical protein subunits has been found in a tyrosyl-tRNA synthetase in solution (Ward & Fersht, 1988). This dimeric enzyme exhibits half-of-the-sites activity. In heterodimers consisting of one full-length and one truncated subunit, an asymmetrical structure was found, where each dimer was active at only one site, but the site used was randomly distributed between the subunits. The subtle, but significant, differences observed in the Zn_A environment upon population of site B with Pb are consistent with the idea that the two sites are able to communicate with each other through either close proximity or some allosteric effect.

ACKNOWLEDGMENTS

We thank Dr. R. W. Strange for assistance with the data collection and especially for advice to A.J.D. on the analysis of the data. The spectrum of bis(thiourea)zinc acetate was kindly provided by Dr. G. P. Diakun. We express our thanks to reviewer 2 for his constructive suggestions.

Registry No. ALAD, 9036-37-7; Zn, 7440-66-6.

REFERENCES

Arber, J. M., de Boer, E., Garner, C. D., Hasnain, S. S., & Wever, R. (1989) *Biochemistry 28*, 7968–7973.

Barnard, G. F., Itoh, R., Hohberger, L. H., & Shemin, D. (1977) *J. Biol. Chem. 252*, 8965–8974.

Batlle, A. M. d. C., Ferramola, A. M., & Grinstein, M. (1967) *Biochem. J. 104*, 244–249.

Bear, C. A., Duggan, K. A., & Freeman, H. C. (1975) *Acta Crystallogr. B31*, 2713.

Berg, J. M. (1986) *Science 232*, 485–487.

Bevan, D. R., Bodlaender, P., & Shemin, D. (1980) *J. Biol. Chem. 225*, 2030–2035.

Binsted, N., Gurman, S. J., & Campbell, J. W. (1988) SERC Daresbury Laboratory Program, Daresbury Laboratory, Warrington, U.K.

Cavalca, L., Gasparii, G. F., Andreetti, G. D., & Domiano, P. (1967) *Acta Crystallogr. 22*, 90.

Chaudhry, A. G., Gore, M. G., & Jordan, P. M. (1976) *Biochem. Soc. Trans. 4*, 301–303.

Cheh, A., & Neilands, J. B. (1976) *Struct. Bonding (Berlin) 29*, 123–169.

Corwin, D. T., Jr., & Koch, S. A. (1988) *Inorg. Chem. 27*, 493–496.

Garner, C. D., & Feiters, M. C. (1987) in *Biophysics and Synchrotron Radiation* (Bianconi, A., & Congiu-Castellano, A., Eds.) p 136, Springer, Berlin.

Garner, C. D., Hasnain, S. S., Bremner, I., & Bordas, J. (1982) *J. Inorg. Chem. 16*, 253–256.

Garratt, R. C. (1989) Ph.D. Thesis, University of London, Birkbeck College.

Garrett, T. P. J., Guss, J. M., & Freeman, H. C. (1983) *Acta Crystallogr. C39*, 1027–1031.

Gurman, S. J., & Pendry, J. B. (1976) *Solid State Commun. 28*, 287–290.

Gurman, S. J., Binsted, N., & Ross, I. (1984) *J. Phys. C 17*, 143–151.

Gurman, S. J., Binsted, N., & Ross, I. (1986) *J. Phys. C 19*, 1845–1861.

Hasnain, S. S., & Strange, R. W. (1989) in *Biophysics and Synchrotron Radiation* (Hasnain, S. S., Ed.) Chapter 4, Ellis Horwood Ltd., Chichester, U.K.

Hasnain, S. S., Quinn, P. D., Diakun, G. P., Wardell, E. M., & Garner, C. D. (1984) *J. Phys. E 17*, 40–43.

Hasnain, S. S., Wardell, E. M., Garner, C. D., Schlösser, M., & Beyersmann, D. (1985) *Biochem. J. 230*, 633–635.

Hasnain, S. S., Strange, R. W., Diakun, G. P., Jones, G., & Campbell, J. W. (1988) in *Abstracts of the 2nd International Conference on Biophysics and Synchrotron Radia-*

tion, pp 91-93, Chester, U.K. Daresbury Laboratory, Warrington, U.K.
Jaffe, E. K., & Hanes, D. (1986) *J. Biol. Chem. 261*, 9348-9353.
Jaffe, E. K., Salowe, S. P., Chen, N. T., & De Haven, P. A. (1984) *J. Biol. Chem. 259*, 5032-5036.
Joyner, R. W., Martin, K. J., & Meehan, P. (1987) *J. Phys. C 20*, 4005-4012.
Lowry, O. H., Rosebrough, N. J., Farr, A. L., & Randall, R. J. (1951) *J. Biol. Chem. 193*, 265-275.
Matheis, L. F. (1964) *Phys. Rev. A133*, 1399.
Mauzerall, D., & Granick, S. (1956) *J. Biol. Chem. 219*, 435-446.
Morrel, C., Baines, J. T. M, Campbell, J. W., Diakun, G. P., Dobson, B. R., Greaves, G. N., & Hasnain, S. S. (1989) *Daresbury EXAFS Users' Manual*, Daresbury Laboratory, Warrington, U.K.
Pendry, J. B. (1974) *Low Energy Electron Diffraction*, Academic Press, New York.
Perutz, M. F., Hasnain, S. S., Duke, P. J., Sessler, J. L., & Hahn, J. E. (1982) *Nature 295*, 535-538.
Pilz, I., Schwarz, E., Vuga, M., & Beyersmann, D. (1990) *Biol. Chem. Hoppe-Seyler* (in press).
Schlösser, M., & Beyersmann, D. (1987) *Biol. Chem. Hoppe-Seyler 368*, 1469-1477.
Shemin, D. (1972) *Enzymes (3rd Ed.) 7*, 323-337.
Shemin, D. (1976) *Philos. Trans. R. Soc. London, B 273*, 109-115.
Sommer, R., & Beyersmann, D. (1984) *J. Inorg. Biochem. 20*, 131-145.
Strange, R. W., Blackburn, N. J., Knowles, P. F., & Hasnain, S. S. (1987) *J. Am. Chem. Soc. 109*, 7157-7162.
Tsukamoto, I., Yoshinga, T., & Sano, S. (1979) *Biochim. Biophys. Acta 570*, 167-178.
Tsukamoto, I., Yoshinga, T., & Sano, S. (1980) *Int. J. Biochem. 12*, 751-756.
Ward, W. H. J., & Fersht, A. R. (1988) *Biochemistry 27*, 1041-1049.
Wetmur, J. G., Bishop, D. F., Cantelmo, C., & Desnick, R. J. (1986) *Proc. Natl. Acad. Sci. U.S.A. 83*, 7703-7707.

Conformational Preferences of Synthetic Peptides Derived from the Immunodominant Site of the Circumsporozoite Protein of *Plasmodium falciparum* by ^{1}H NMR†

H. Jane Dyson,* Arnold C. Satterthwait,* Richard A. Lerner, and Peter E. Wright

Department of Molecular Biology, Research Institute of Scripps Clinic, 10666 North Torrey Pines Road, La Jolla, California 92037

Received January 22, 1990; Revised Manuscript Received April 12, 1990

ABSTRACT: Proton nuclear magnetic resonance and ultraviolet circular dichroism spectroscopy have been used to probe the conformational ensemble of the tandemly repeating tetrapeptide unit of the circumsporozoite coat protein of the malaria parasite *Plasmodium falciparum*. Peptides based on the Asn-Ala-Asn-Pro and Asn-Pro-Asn-Ala cadences and composed of one to three tetrapeptide units were synthesized and examined using one- and two-dimensional NMR spectroscopy. The chemical shift of the amide protons, the temperature dependence of the amide proton chemical shift, and the patterns of NOE connectivities in the various peptides give evidence for the presence of a substantial population of folded conformers in several of the peptides in water solution at pH 5.0. Correlations between the behavior of the tandemly repeated units in different peptides have been used to infer the structure(s) of the folded conformers. The data are consistent with the presence of turnlike structures stabilized by hydrogen bonding of the backbone amide protons of the alanines and the asparagine residues preceding them. Specific differences in the strengths of NOEs between peptides of different lengths indicate that the folded structure is considerably stabilized by the presence of the asparagine residue following the alanine. Differences between peptides with different cadences of the tandemly repeating unit indicate that a repeating structural motif is formed by the Asn-Pro-Asn-Ala-(Asn) cadence.

Recent advances in the molecular biology of malaria parasites and new developments in vaccine design have led to vigorous efforts to design effective malaria vaccines (Miller et al., 1986). Synthetic peptide vaccines based on cognate sequences found on the surfaces of sporozoites (Herrington et al., 1987) and merozoites (Patarroyo et al., 1988) have undergone clinical trials and show promise of protection. In order to produce effective vaccines, a strategy of rational design of the peptide immunogens is desirable. One promising approach is the design of peptide immunogens based on the known structure of components of the various forms of the parasite.

In general, peptide vaccines elicit a variety of antibodies, only some of which may bind tightly to the cognate sequence in the native protein or the pathogen. This is presumably due to the variety of conformers accessible to small, flexible peptides. If the structure of the conformer which induces protein-reactive antibodies could be determined, then it should

† This research was supported by Grant PO1 CA27498 from the National Institutes of Health and by the MacArthur Foundation.
* Address correspondence to these authors.

0006-2960/90/0429-7828$02.50/0